

Effects of Doxorubicin, Cisplatin, and Tamoxifen on the Metabolic Profile of Human Breast Cancer MCF-7 Cells As Determined by ^1H High-Resolution Magic Angle Spinning Nuclear Magnetic Resonance

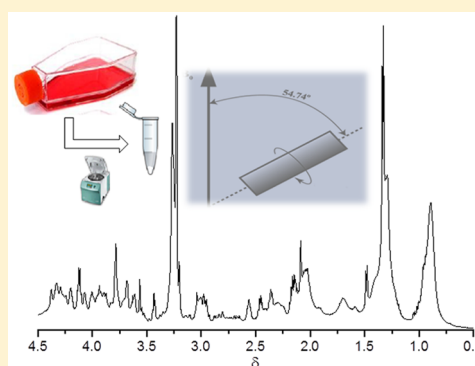
Roberta M. Maria,[†] Wanessa F. Altei,[‡] Heloisa S. Selistre-de-Araujo,[‡] and Luiz A. Colnago^{*,†}

[†]Embrapa Instrumentação, Rua XV de Novembro, 1452, São Carlos, SP 13560-970, Brazil

[‡]Laboratório de Bioquímica e Biologia Molecular, Departamento de Ciências Fisiológicas, Universidade Federal de São Carlos (UFSCar), Rodovia Washington Luís, km 235, Caixa Postal 676, São Carlos, SP 13565-905, Brazil

Supporting Information

ABSTRACT: Doxorubicin (Doxo), cisplatin (Cis), and tamoxifen (Tamo) are part of many chemotherapeutic regimens. However, there have been limited studies of the way metabolism in breast cancer is affected by chemotherapy. We studied, through ^1H high-resolution magic angle spinning nuclear magnetic resonance (HR-MAS NMR) spectroscopy, the metabolic profile of human breast cancer MCF-7 control (Con) cells as well as MCF-7 cells treated with Tamo, Cis, and Doxo. ^1H HR-MAS NMR single-pulse spectra evidenced signals from the cell compounds, including fatty acids (membranes), water-soluble proteins, and metabolites. The spectra showed that phosphocholine (i.e., biomarker of breast cancer malignant transformation) signals were stronger in Con than in treated cells. Betaine (i.e., the major osmolyte in cells) was observed at similar concentrations in MCF-7 control and treated cells but was absent in nontumor MCF-10A cells. The NMR spectra acquired with the Carr–Purcell–Meiboom–Gill (CPMG) pulse sequence were used only in qualitative analyses because the signal areas were attenuated according to their transverse relaxation time (T_2). The CPMG method was used to identify soluble metabolites such as organic acids, amino acids, choline and its derivatives, taurine, and guanidino acetate. ^1H HR-MAS NMR spectroscopy efficiently demonstrated the effects of Tamo, Cis, and Doxo on the metabolic profile of MCF-7 cells. The fatty acid, phosphocholine, and choline variations observed by single-pulse HR-MAS NMR have the potential to characterize both responder and nonresponder tumors at a molecular level.



Chemotherapy has improved relapse-free and overall survival times in women with locally advanced breast cancer.¹ Doxorubicin, cisplatin, and tamoxifen are among the frequently used drugs in cancer chemotherapy.

Doxorubicin corresponds to a class of compounds featuring similar structures, the so-called anthracyclines.² The cytostatic effect of this drug may involve several mechanisms, such as inhibition of both topoisomerase II and RNA polymerase II.³ The formation of reactive oxygen species (ROS), intercalation of doxorubicin into chromosomal DNA, and generation of complexes with iron have also been attributed to the doxorubicin cytostatic mechanism.³ Doxorubicin is considered one of the most efficient approaches for the treatment of breast cancer, even though its resistance has led to an unsuccessful outcome in many patients.⁴

Cisplatin is another compound used in cancer chemotherapy. It frequently promotes a prompt satisfying response.⁵ Cisplatin consists of an inorganic platinum complex that inhibits DNA synthesis. However, the resistance of tumor cells to cisplatin has been a fundamental problem in tumor management, being responsible for the collapse of metastatic cancer treatment.⁶ Likewise, cisplatin cytotoxicity to regular tissues as well as the

resistance of cancer cells to this compound impairs the therapeutic response.^{7,6}

Tamoxifen is a nonsteroidal antiestrogen that was first approved by the U.S. Food and Drug Administration (FDA) in 1977 for metastatic breast cancer treatment.^{8,9} This chemotherapeutic compound has also been used to reduce the recurrence of primary breast cancer and contributes to survival rates as an adjuvant treatment.^{9,8}

Tumor biomarkers have been used to establish the disease stage and the efficacy of different drugs and doses.¹⁰ Biomarkers can also be used to discriminate between “responders” and “non-responders”.¹⁰ In the past decade, metabolomic biomarkers have been combined with radiological, genomic, and proteomic ones to establish the tumor stage. Metabolomics, which stands for the overall assessment of endogenous metabolites within a biological system,¹⁰ has become more frequently used to study the effects of anticancer drugs on tumor cells.⁴

Received: January 10, 2017

Revised: March 29, 2017

Published: April 5, 2017

Nuclear magnetic resonance (NMR) spectroscopy and mass spectrometry denote the conventional methods used in metabolomic studies. Numerous NMR metabolomic protocols rely upon the analysis of tumor extracts that destroy the sample. On the other hand, ^1H high-resolution magic angle spinning (^1H HR-MAS) NMR spectroscopy^{11,12} has been used to study the metabolic profile of cancer cells and tissues collected through biopsies, without cellular lysis. ^1H HR-MAS also provides rapid, highly accurate, and reproducible analyses requiring straightforward sample preparation.^{12,13}

In this work, the effects of doxorubicin, cisplatin, and tamoxifen on the metabolic profile of intact human breast cancer MCF-7 cells were studied by ^1H HR-MAS NMR. MCF-7 cells are known to grow in a highly hormone-dependent fashion as well as to form well-differentiated tumors in a xenograft animal experimental model.¹⁴ The results confirmed that all drugs have strong effects on the metabolite profile. The major effects were decreases in phosphocholine and fatty acid contents, which are considered a biomarker in breast cancer malignant transformation and the primary material of cell membrane assembly in fast-growing cells, respectively.

MATERIALS AND METHODS

Sample Preparation. MCF-10A (ATCC CRL-10371) (mammary gland breast nontumorigenic cell line) and MCF-7 (ATCC HTB 22) (human breast cancer cell line, estrogen receptor-positive) cells were obtained from the Rio de Janeiro cell collection (BCRJ, Rio de Janeiro, Brazil). MCF-10A was maintained in Dulbecco's modified Eagle's medium: nutrient mixture F-12 (DMEM/F-12) (Invitrogen Co., Carlsbad, CA) supplemented with 5% fetal horse serum (Thermo Fisher Scientific Inc.), 1% penicillin/streptomycin (Thermo Fisher Scientific Inc.), 10 $\mu\text{g}/\text{mL}$ bovine insulin (Sigma-Aldrich), 20 ng/mL epidermal growth factor (EGF) (Sigma-Aldrich), and 0.5 mg/mL hydrocortisone (Sigma-Aldrich). All cells were maintained at 37 °C in a humidified atmosphere comprising 95% air and 5% CO_2 .

MCF-7 cells were grown in Roswell Park Memorial Institute medium (RPMI) (Thermo Fisher Scientific Inc., Waltham, MA) supplemented with 10% heat-inactivated fetal bovine serum (FBS) (Thermo Fisher Scientific Inc.). Cells were seeded at a density of 1.4×10^6 cells per 75 cm^2 cell culture flask and maintained at 37 °C in a humidified incubator containing 5% CO_2 for 72 h to allow cells to attach to the flask and become confluent. The medium was removed, and subcultures were obtained by treating cells with trypsin in phosphate-buffered saline (PBS) (Sigma-Aldrich) for 2 min. Subsequently, 4 mL of culture medium were added, and cells were centrifuged at 1200 rpm for 5 min to form pellets. After centrifugation, 10 μL of D_2O was added to approximately 40 μL of a MCF-7 pellet in PBS. This procedure was performed in triplicate. Cell viability was tested by Trypan Blue exclusion prior to the measurements.

Supplementation of MCF-7 Cells. MCF-7 cells were cultured as described above. After confluence, cells were treated with the drugs (i.e., doxorubicin, cisplatin, and tamoxifen), individually, for 24 h. The culture medium was supplemented with 1 μM doxorubicin, 70 μM cisplatin, and 25 μM tamoxifen. We relied upon previous cytotoxicity assays with doxorubicin,¹⁵ cisplatin,¹⁶ and tamoxifen¹⁵ to choose such drug concentrations. Cells treated with cisplatin, tamoxifen, and doxorubicin were detached from the culture flask using trypsin. Once centrifuged, the pellets were resuspended in D_2O and newly

centrifuged prior to NMR analysis. This procedure was performed in triplicate for each drug.

^1H HR-MAS NMR Analyses. Each of the formed pellets was packed into a zirconium HR-MAS rotor containing 10 μL of deuterium oxide with sodium trimethylsilyl-[2,2,3,3- $^2\text{H}_4$]-1-propionate (TMSP). The system was adjusted to 0.00 ppm, whereas the spin was set to the magic angle (i.e., 54.7° relative to the magnetic field z direction). ^1H HR-MAS spectroscopy was performed at 14.1 T (600 MHz for ^1H) and a 5 kHz spinning rate using an AVANCE 600 BRUKER NMR spectrometer. The spectra were recorded with a 1.5 s presaturation pulse, an acquisition time of 4.63 s (32K points), a 4 s recycle delay, and an accumulation of 256 transients. Additionally, a Carr–Purcell–Meiboom–Gill (CPMG) spin–echo train was employed before data acquisition by means of applying 120 cycles separated by 1.2 ms echoes. The FID signal was multiplied by a 1.0 Hz (0.0025 ppm) line broadening as well as a zero-filled 2-fold for Fourier transformation. For automatic phase adjustment and baseline correction, the Advanced Chemistry Development (ACD) Laboratories software was applied. Samples were also analyzed using two-dimensional (2D) NMR spectroscopy methods, such as COSY (correlation spectroscopy), ^1H – ^{13}C HSQC (proton–carbon heteronuclear single-quantum correlation spectroscopy), and ^1H – ^{13}C HMBC (proton–carbon heteronuclear multiple-bond correlation spectroscopy). ^1H HR-MAS spectra of cancer cells were assigned using correlated spectroscopy (2D homonuclear and heteronuclear NMR experiments, including COSY, ^1H – ^{13}C HSQC, and ^1H – ^{13}C HMBC). Online databases, such as the Human Metabolome Database (HMDB) and Chemomx, were also suitable for assignments. One-dimensional (1D) ^1H HR-MAS spectra were normalized by correcting the baseline offset to zero and by dividing each data point by the sum of all data points, values that were multiplied by 1000.

RESULTS

Figures 1 and 2 show the ^1H HR-MAS NMR spectra of human breast cancer MCF-7 control cells (Con) and MCF-7 cells treated with tamoxifen (Tamo), cisplatin (Cis), and doxorubicin (Doxo). The spectra shown in Figure 1 were acquired with a single pulse, whereas those presented in Figure 2 were recorded with the CPMG pulse sequence. The single-pulse spectra (Figure 1) show the signals from the compounds in the cells, including fatty acids (membranes) as well as some water-soluble proteins and metabolites. The spectra acquired with the CPMG sequence (Figure 2) show only the sharp signals of the water-soluble metabolites. The CPMG sequence itself has been used as a transverse relaxation time (T_2) filter (T_2 filter) and been shown to be more efficient in attenuating broad (shorter T_2) rather than sharp (longer T_2) signals. Therefore, all signals presented in Figure 2 were attenuated according to their T_2 values as well as the total echo time used in the CPMG sequence. Consequently, the CPMG spectra (Figure 2) can be used only in qualitative analyses.

Figures 1A–D and 2A–D present the single-pulse and CPMG ^1H HR-MAS NMR spectra, respectively, from 0.5 to 4.5 ppm, of Con (A), Tamo (B), Cis (C), and Doxo (D). Figures 1A'–D' and 2A'–D' show the single-pulse and CPMG ^1H HR-MAS NMR spectra, respectively, of the same samples [i.e., Con (A'), Tamo (B'), Cis (C'), and Doxo (D')], from 5.0 to 10.0 ppm. The vertical axes of spectra A'–D' were 4-fold magnified. Both single-pulse and CPMG ^1H HR-MAS NMR

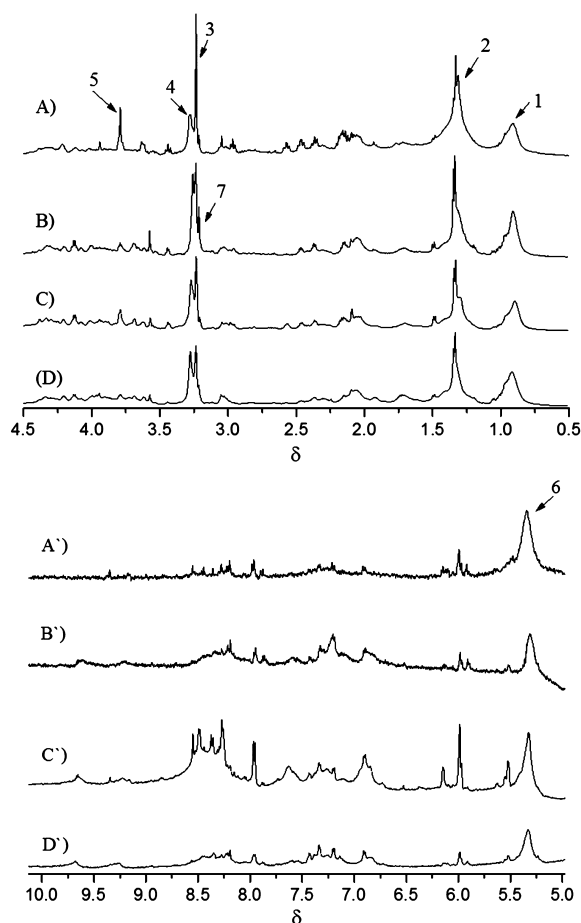


Figure 1. Single-pulse ^1H HR-MAS NMR normalized spectra of human breast cancer MCF-7 cells. Spectra of control cells (A and A') and cells treated with Tamo (B and B'),¹⁵ Cis (C and C'),¹⁶ and Doxo (D and D')¹⁵ are shown. The vertical axes of spectra A'–D' were 4-fold magnified. The numbers indicate the assignments to methyl (1) and methylene groups (2) of fatty acids and proteins; to phosphocholine (3), betaine (4), and guanidino acetate (5); and to olefinic hydrogens of unsaturated fatty acids (6) and choline (7). Spectra A–D are from 0.5 to 4.5 ppm, whereas spectra A'–D' are from 5.0 to 10.0 ppm. See also [Figure S1](#).

spectra of the three cultures for each treatment (triplicates) are shown in [Figures S1 and S2](#).

Spectral Assignments. All spectra of [Figure 1](#) show strong, broad peaks overlapped with sharp, weak peaks, the latter being assigned to water-soluble metabolites. The broad, strong peaks at 0.9 ppm (1) and 1.3 ppm (2) have been assigned to methyl and methylene groups of fatty acids and proteins, respectively. These peaks also comprised signals from metabolites that were better resolved in [Figure 2](#). The broad peak at 5.3 ppm (6) has been assigned to the olefinic hydrogens of unsaturated fatty acids. The Con spectrum ([Figure 1A](#)) also exhibited strong peaks at 3.22 ppm (3), 3.26 ppm (4), and 3.78 ppm (5), which have been assigned to phosphocholine, betaine, and guanidino acetate, respectively. The Tamo spectrum ([Figure 1B](#)) showed a strong choline peak at 3.20 ppm (7).

[Figure 2](#) shows the assignment of 16 metabolites: lactate/threonine (1/2), alanine (3), acetate (4), glutamate/glutamine (5/6), acetone (7), creatine (8), choline (9), phosphocholine (10), taurine (11), glycine (12), guanidino acetate (13), UTP/UDP/UMP (14), tyrosine (15), and phenylalanine (16).

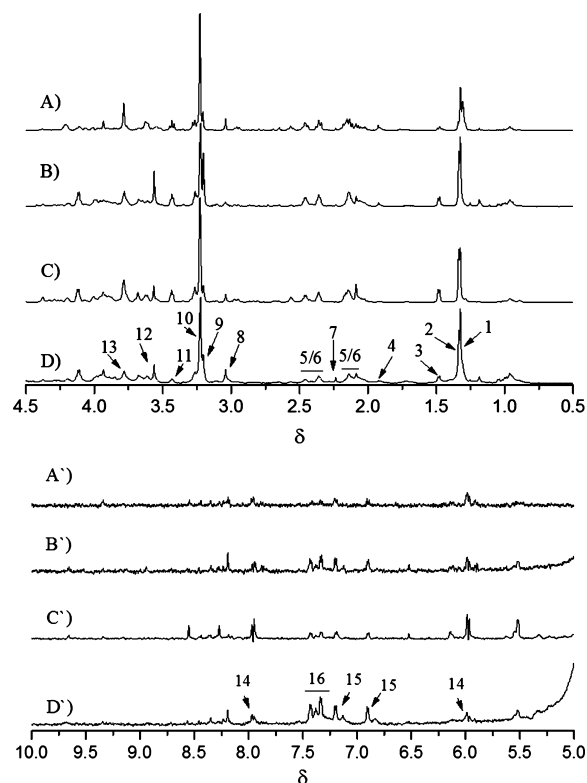


Figure 2. ^1H HR-MAS NMR spectra of the following breast cancer MCF-7 cells, acquired with the CPMG pulse sequence: MCF-7 control cells (A and A') and MCF-7 cells treated with Tamo (B and B'),¹⁵ Cis (C and C'),¹⁶ and Doxo (D and D').¹⁵ The vertical axes of spectra A'–D' were 4-fold magnified. The numbers indicate peaks attributed to lactate/threonine (1/2), alanine (3), acetate (4), glutamate/glutamine (5/6), acetone (7), creatine (8), choline (9), phosphocholine (10), taurine (11), glycine (12), guanidino acetate (13), UTP/UDP/UMP (14), tyrosine (15), and phenylalanine (16). Spectra A–D are from 0.5 to 4.5 ppm, whereas spectra A'–D' are from 5.0 to 10.0 ppm. See also [Figure S2](#).

Lactate, threonine, alanine, acetate, glutamate, and glutamine were attributed to signals at 1.32 ppm (1), 1.33 ppm (2), 1.47 ppm (3), and 1.91 ppm (4) as well as from 2.0 to 2.5 ppm (5 and 6), respectively. The signal at 2.2 ppm (7) was assigned to acetone and corroborated by the HSQC (^1H – ^{13}C) signal at 32.86 ppm as well as the HMBC signal at 217.95 ppm ($\text{C}=\text{O}$). Creatine (8) was assigned to the signal at 3.03 ppm. Choline (9) was assigned to the signal at 3.20 ppm ($\text{N}-\text{CH}_3$) and correlated with HSQC (^1H – ^{13}C), at 56.64 ppm ($\text{N}-\text{CH}_3$), and with HMBC, at 70.29 ppm (βCH_2). Phosphocholine (10) was attributed to the signal at 3.22 ppm ($\text{N}-\text{CH}_3$) with ^1H – ^{13}C correlations in the HSQC spectrum at 56.62 ppm ($\text{N}-\text{CH}_3$) as well as in the HMBC spectrum at 69.19 ppm (βCH_2) and 59.63 ppm ($\text{C}-\text{O}$). Taurine (11) was assigned to the signal at 3.42 ppm (βCH_2). Taurine triplets ($J = 6.47$ Hz) were also clearly separated in the J-resolved spectrum. Glycine (12) was attributed to the signal at 3.55 ppm, whereas guanidino acetate (13) was assigned to that at 3.78 ppm. UTP/UDP/UMP (14) was assigned to the signals at 5.98 and 7.94 ppm. Finally, tyrosine (15) was assigned to the signals at 6.90 and 7.18 ppm, while phenylalanine (16) was attributed to those at 7.31, 7.36, and 7.41 ppm. See also [Figure S3](#) and [Table S4](#).

Effect of Chemotherapeutic Drugs on the ^1H HR-MAS NMR Spectra of MCF-7 Cells. The area below the single-pulse ^1H HR-MAS NMR spectra ([Figure 1](#)) shows the

following variations. Peak 1 was larger in Tamo > Con > Cis ~ Doxo. Peaks 2 and 3 were larger in Con > Tamo > Cis ~ Doxo. Peak 4 was similar in all treatments. Peak 5 was larger in Con > Cis > Tamo ~ Doxo. Peak 6 was larger in Con ~ Cis > Tamo ~ Doxo. Peak 7 was larger in Tamo > Con ~ Cis ~ Doxo. Therefore, the spectrum of control cells showed the highest content of phosphocholine and unsaturated fatty acids (peaks 3 and 6, respectively), which is in accordance with previous reports found in the literature.¹⁷ Phosphocholine has been considered as a biomarker of breast cancer malignant transformation, and the growing tumor cells need higher fatty acid contents to form cell membranes.^{18,17}

The Tamo spectrum shows peaks 1, 2, and 7 that are stronger than those of Cis and Doxo. Larger areas corresponding to methyl (1) and methylene (2) groups as well as a smaller area assigned to olefinic hydrogens (6) indicate that Tamo either induced the synthesis or reduced the rate of uptake of saturated fatty acids. The higher content of choline (7) also indicates that this drug strongly interfered in the phosphatidylcholine metabolism (Kennedy pathway).^{10,19} The spectra of Cis and Doxo suggest that these drugs have strong effects on MCF-7 cell metabolism, taking into account that most of the metabolites were present at low concentrations. The spectra of drug-treated cells showed contents of aromatic compounds such as tyrosine, phenylalanine, and UTP/UDP/UMP (signal from 6.5 to 10 ppm) higher than those of control cells (Figure 1A').

The cells treated with Cis show the strongest signals in the aromatic region compared with Doxo and Tamo treatments. Cisplatin is considered as a DNA-damaging anticancer drug.^{6,20} Additionally, cisplatin cause damage in tumors via induction of apoptosis, mediated by the activation of various signal transduction pathways, for example, disruption of intracellular calcium homeostasis,²⁰ death receptor signaling, and activation of mitochondrial pathways.⁶ In particular, the activation of mitochondrial pathways can explain the higher concentration of UMP/UDP/UTP observed in the spectra of cisplatin-treated MCF-7 cells. The significant presence of UMP/UDP/UTP can result from the intervention of cisplatin in bioenergetic features of mitochondria in MCF-7 cells. Probably, with the influence on many biochemical pathways, cisplatin (platinum compound) may alter the metabolism and/or catabolism of aromatic amino acids, such as phenylalanine and tyrosine.

Peak 4 at 3.26 ppm, assigned to methyl groups of betaine, was similar in all MCF-7 cell samples. However, it was absent in the single-pulse ¹H HR-MAS NMR spectrum of nontumor MCF-10A cells (inset in Figure 3). In the MCF-10A spectrum (Figure 3), the broad peak attributed to fatty acids was remarkably weak; on the other hand, the phosphocholine signal was absent, and the major metabolites were glucose, ethanol, lactate, acetate, asparagine, and ethanolamine.²⁷

Betaine is a major osmolyte in cells and plays an essential role in cellular protection against environmental stress, including high temperature and osmotic imbalance.²¹ It also regulates the cell volume and stabilizes proteins.²² Therefore, the presence of betaine in both untreated (control) and treated MCF-7 cells but not in MCF-10A cells corroborates the stress condition experienced by tumor cells.

The areas under CPMG ¹H HR-MAS NMR signals (Figure 2) of lactate (1), threonine (2), alanine (3), and glycine (12) in untreated cells (Con) were found to be smaller than in their treated counterparts. Phosphocholine (10) and guanidino acetate (13) were present at higher concentrations in Con

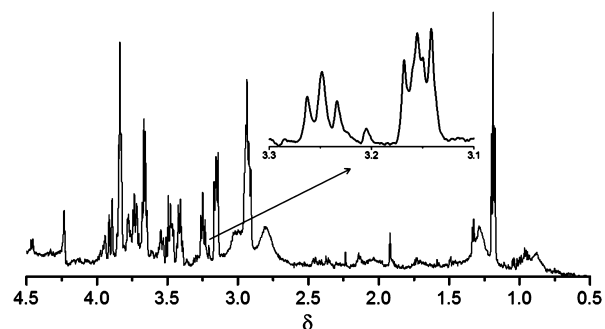


Figure 3. Single-pulse ¹H HR-MAS NMR spectrum of nontumor MCF-10A cells from 0.5 to 4.5 ppm. The inset from 3.1 to 3.3 ppm demonstrates the absence of the peak at 3.26 ppm, assigned to betaine.

and Cis cells, whereas choline (9) and glycine (12) contents were higher in Tamo cells (Figure 2B). Doxo cells showed the lowest phosphocholine content as shown in the single-pulse spectrum (Figure 1D). Because phosphocholine is considered as a biomarker of breast cancer malignant transformation, Doxo was more efficient than Tamo and Cis in reducing the content of this metabolite.

Figures 1A'–D' and 2A'–D' show that Con cells presented the lowest metabolite concentrations, between 5 and 10 ppm. Cis cells (Figures 1C' and 2C') showed higher concentrations of UTP/UDP/UMP (14), tyrosine (15), and phenylalanine (16) than Tamo and Doxo cells did (Figures 1B'–D' and 2B'–D').

DISCUSSION

The higher concentrations of unsaturated fatty acids in Con cells (Figure 1A') than in nontumor cells (Figure 3), as indicated by peak 6, are in line with the high activity of fatty acid synthase in tumor tissue, which in turn is associated with proliferation and malignant transformation.¹⁷ Essentially, the fatty acid synthase activity supports cancer growth by means of increasing the number of building blocks for cell membranes and for lipids containing molecules involved in cell signaling.²³ As a result, it would be possible that fatty acids are synthesized *de novo* in tumor cells themselves.²⁴ Doxo and Tamo were shown to be more efficient than Cis in reducing unsaturated fatty acid content (Figure 1A'–D', peak 6) in cells. Because broad peaks 1 and 2, which are also related to fatty acids, are stronger in Tamo-treated cells than in Cis- and Doxo-treated cells, this drug is believed to induce the synthesis of saturated fatty acids, as suggested by weak peak 6. It has been observed that the liver of rats, upon long-term exposure to tamoxifen, comprised increased contents of choline and fatty acids when compared to those of control cells.²⁵

The area of the phosphocholine signal at 3.22 ppm (Figure 1) was reduced in cells treated with the three drugs. Because phosphocholine is considered as a breast cancer malignant transformation biomarker,¹⁸ this indicates that all drugs reduced its level of synthesis and, as a consequence, cell invasiveness.

The spectra presented in Figure 2 show that the drugs neither strongly affected the concentration of small metabolite molecules nor restored the high glucose level observed in nontumor MCF-10A cells. It is known that cancer cells typically exhibit rates of glucose uptake and consumption higher than those of nontumor cells.²⁶ Tumor cells, even at normal oxygen concentrations, metabolize glucose anaerobically and form

lactate.¹⁰ This explains the larger area assigned to lactate observed in MCF-7 cells upon comparison with that in MCF-10A cells.²⁷ However, the area attributed to lactate in untreated cells (Con) was smaller than in treated cells (Figure 2). This suggests the large disturbance of glycolysis after therapeutic intervention; because lactate is the final product of glycolysis, its accumulation implies an increase in the level of anaerobic glycolysis.

In summary, the NMR spectra acquired with the CPMG pulse sequence were used only in qualitative analyses because the areas under the signals were attenuated by the transverse relaxation time (T_2). The CPMG method was used to identify soluble metabolites (e.g., organic acids, amino acids, choline and its derivatives, taurine, and guanidino acetate). ¹H HR-MAS NMR spectroscopy was remarkably efficient in demonstrating the effects of tamoxifen, cisplatin, and doxorubicin on the metabolic profile of MCF-7 cells. In conclusion, we demonstrated here that the variations in fatty acids, phosphocholine, and choline observed by single-pulse HR-MAS NMR spectroscopy have potential to characterize the responder and nonresponder tumors at the molecular level.

■ ASSOCIATED CONTENT

● Supporting Information

The Supporting Information is available free of charge on the ACS Publications website at DOI: 10.1021/acs.biochem.7b00015.

Single-pulse ¹H HR-MAS NMR normalized triplicate spectra of human breast cancer MCF-7 cells (control cells), single-pulse ¹H HR-MAS NMR normalized triplicate spectra of human breast cancer MCF-7 cells treated with tamoxifen, single-pulse ¹H HR-MAS NMR normalized triplicate spectra of human breast cancer MCF-7 cells treated with cisplatin, single-pulse ¹H HR-MAS NMR normalized triplicate spectra of human breast cancer MCF-7 cells treated with doxorubicin, CPMG ¹H HR-MAS NMR normalized triplicate spectra of human breast cancer MCF-7 cells (control cells), CPMG ¹H HR-MAS NMR normalized triplicate spectra of human breast cancer MCF-7 cells treated with tamoxifen, CPMG ¹H HR-MAS NMR normalized triplicate spectra of human breast cancer MCF-7 cells treated with cisplatin, CPMG ¹H HR-MAS NMR normalized triplicate spectra of human breast cancer MCF-7 cells treated with doxorubicin, 2D spectra with ¹H and ¹³C (J^1) correlations obtained from the HSQC experiment, and assignment of ¹H and ¹³C peaks identified in HQSC experiments with Chenomx (PDF)

■ AUTHOR INFORMATION

Corresponding Author

*E-mail: luiz.colnago@embrapa.br. Fax: +55 16 21072800.

ORCID

Roberta M. Maria: 0000-0002-2390-1843

Funding

We acknowledge the financial support of the Brazilian agencies FAPESP (Grants 2013/05128-5 and 2013/00798-2) and CNPq (Grant 303837/2013-6).

Notes

The authors declare no competing financial interest.

■ REFERENCES

- (1) Rieber, a, Zeitler, H., Rosenthal, H., Görlich, J., Kreienberg, R., Brambs, H. J., and Tomczak, R. (1997) MRI of breast cancer: influence of chemotherapy on sensitivity. *Br. J. Radiol.* 70, 452–8.
- (2) Yang, F., Teves, S. S., Kemp, C. J., and Henikoff, S. (2014) Doxorubicin, DNA torsion, and chromatin dynamics. *Biochim. Biophys. Acta, Rev. Cancer* 1845, 84–89.
- (3) Müller, I., Jenner, a, Bruchelt, G., Niethammer, D., and Halliwell, B. (1997) Effect of concentration on the cytotoxic mechanism of doxorubicin–apoptosis and oxidative DNA damage. *Biochem. Biophys. Res. Commun.* 230, 254–257.
- (4) Smith, L. (2006) The analysis of doxorubicin resistance in human breast cancer cells using antibody microarrays. *Mol. Cancer Ther.* 5, 2115–2120.
- (5) Liang, S., Peng, X., Li, X., Yang, P., Xie, L., Li, Y., Du, C., and Zhang, G. (2015) Silencing of CXCR4 sensitizes triple-negative breast cancer cells to cisplatin. *Oncotarget* 6, 1020–1030.
- (6) Florea, A.-M., and Büsselberg, D. (2011) Cisplatin as an Anti-Tumor Drug: Cellular Mechanisms of Activity, Drug Resistance and Induced Side Effects. *Cancers* 3, 1351–1371.
- (7) Skolekova, S., Matuskova, M., Bohac, M., Toro, L., Durinikova, E., Tyciakova, S., Demkova, L., Gursky, J., and Kucerova, L. (2016) Cisplatin-induced mesenchymal stromal cells-mediated mechanism contributing to decreased antitumor effect in breast cancer cells. *Cell Commun. Signaling* 14, 4.
- (8) Wiebe, V. J., Osborne, C. K., Fuqua, S. a. W., and DeGregorio, M. W. (1993) Tamoxifen resistance in breast cancer. *Crit. Rev. Oncol. Hematol.* 14, 173–188.
- (9) Hertl, M., and Cosimi, A. B. (2007) Oncologist. *Liver Transplantation*, 4–11.
- (10) Merz, A., and Serkova, N. J. (2009) Use of NMR-based metabolomics in detecting drug resistance in cancer. *Biomarkers Med.* 3, 289–306.
- (11) Sitter, B., Bathen, T. F., Tessem, M.-B., and Gribbestad, I. S. (2009) High-resolution magic angle spinning (HR MAS) MR spectroscopy in metabolic characterization of human cancer. *Prog. Nucl. Magn. Reson. Spectrosc.* 54, 239–254.
- (12) Palmnas, M., and Vogel, H. (2013) The Future of NMR Metabolomics in Cancer Therapy: Towards Personalizing Treatment and Developing Targeted Drugs? *Metabolites* 3, 373–396.
- (13) Ferretti, a, Knijn, a, Iorio, E., Pulciani, S., Giambenedetti, M., Molinari, a, Meschini, S., Stringaro, a, Calcabrini, a, Freitas, I., Strom, R., Arancia, G., and Podo, F. (1999) Biophysical and structural characterization of ¹H-NMR-detectable mobile lipid domains in NIH-3T3 fibroblasts. *Biochim. Biophys. Acta, Mol. Cell Biol. Lipids* 1438, 329–48.
- (14) Bando, H., Toi, M., Kitada, K., and Koike, M. (2003) Genes commonly upregulated by hypoxia in human breast cancer cells MCF-7 and MDA-MB-231. *Biomed. Pharmacother.* 57, 333–340.
- (15) Abu, N., Akhtar, M. N., Ho, W. Y., Yeap, S. K., and Alitheen, N. B. (2013) 3-Bromo-1-hydroxy-9,10-anthraquinone (BHAQ) inhibits growth and migration of the human breast cancer cell lines MCF-7 and MDA-MB231. *Molecules* 18, 10367–77.
- (16) Tassone, P., Tagliaferri, P., Perricelli, a, Blotta, S., Quaresima, B., Martelli, M. L., Goel, a, Barbieri, V., Costanzo, F., Boland, C. R., and Venuta, S. (2003) BRCA1 expression modulates chemosensitivity of BRCA1-defective HCC1937 human breast cancer cells. *Br. J. Cancer* 88, 1285–1291.
- (17) Milgraum, L. Z., Witters, L. A., Pasternack, G. R., and Kuhajda, F. P. (1997) Enzymes of the Fatty Acid Synthesis Pathway are highly expressed in situ breast carcinoma. *Clin. Cancer Res.* 3, 2115–2120.
- (18) Eliyahu, G., Kreizman, T., and Degani, H. (2007) Phosphocholine as a biomarker of breast cancer: molecular and biochemical studies. *Int. J. Cancer* 120, 1721–30.
- (19) Glunde, K., Bhujwalla, Z. M., and Ronen, S. M. (2011) Choline metabolism in malignant transformation. *Nat. Rev. Cancer*, 835–848.
- (20) Al-Taweel, N., Varghese, E., Florea, A.-M., and Büsselberg, D. (2014) Cisplatin (CDDP) triggers cell death of MCF-7 cells following

disruption of intracellular calcium ($[Ca^{2+}]_i$) homeostasis. *J. Toxicol. Sci.* 39, 765–774.

(21) Lee, I. (2015) Betaine is a positive regulator of mitochondrial respiration. *Biochem. Biophys. Res. Commun.* 456, 621–625.

(22) Obeid, R. (2013) The metabolic burden of methyl donor deficiency with focus on the betaine homocysteine methyltransferase pathway. *Nutrients* 5, 3481–3495.

(23) Buzzai, M., Bauer, D. E., Jones, R. G., DeBerardinis, R. J., Hatzivassiliou, G., Elstrom, R. L., and Thompson, C. B. (2005) The glucose dependence of Akt-transformed cells can be reversed by pharmacologic activation of fatty acid β -oxidation. *Oncogene* 24, 4165–4173.

(24) Beckonert, O., Monnerjahn, J., Bonk, U., and Leibfritz, D. (2003) Visualizing metabolic changes in breast-cancer tissue using 1H -NMR spectroscopy and self-organizing maps. *NMR Biomed.* 16, 1–11.

(25) Schnackenberg, L., Beger, R. D., and Dragan, Y. (2005) NMR-based metabolomic evaluation of livers from rats chronically treated with tamoxifen, mestranol, and phenobarbital. *Metabolomics* 1, 87–94.

(26) Glunde, K., Jiang, L., Moestue, S. A., and Gribbestad, I. S. (2011) MRS and MRSI guidance in molecular medicine: Targeting and monitoring of choline and glucose metabolism in cancer. *NMR Biomed.* 24, 673–690.

(27) Maria, R. M., Altei, W. F., Andricopulo, A. D., Becceneri, A. B., Cominetti, M. R., Venâncio, T., and Colnago, L. A. (2015) Characterization of metabolic profile of intact non-tumor and tumor breast cells by high-resolution magic angle spinning nuclear magnetic resonance spectroscopy. *Anal. Biochem.* 488, 14–18.